

## CHAPTER IV

### STATHMIN EXPRESSION AND DIFFERENTIAL PHOSPHORYLATION PROMOTE PROSTATE CANCER PROGRESSION

Stathmin is a highly conserved protein and the N-terminal has four serine residues which are phosphorylated by diverse groups of extracellular factors in mammalian cells (128), suggesting that stathmin participates as a “relay protein” in several intracellular signaling pathways (99). The first pathway involves PAK1 and  $Ca^{2+}$ /calmodulin dependent kinase, which phosphorylate stathmin at serine 16 (ser16) (129). Phosphorylation by PAK1 requires Rac/Cdc42 and has been shown to inhibit stathmin-induced destabilization of microtubules, thereby regulating F-actin and microtubule dynamics (129, 130). The second pathway involves Mitogen Activated Protein (MAP) kinase ERK2 which when triggered by growth factor receptors, phosphorylates stathmin at Ser25 (131, 132). A Ser25 to alanine mutation blocks phosphorylation and inhibits cell growth in leukemic K562 cells (133). A third pathway involves Cyclin dependent Kinase 1 (CDK1) which phosphorylates stathmin at Ser38 (134). Inhibition of Ser38 phosphorylation blocks cell division and induces a  $G_2/M$  block in K562 cells (135). Phosphorylation of stathmin at Ser63 by Protein Kinase A (PKA) represents the fourth pathway (136) and a Ser63 to alanine mutation, which prevents phosphorylation at this residue, results in microtubule destabilization and a cell cycle arrest in K562 cells (137, 138). At this time it is not clear which of these pathways is involved in promoting PCa.

## Stathmin is elevated during PIN and adenocarcinoma development in the NeoTag tissue recombination model

Cell lines that express stathmin *in vitro* and recapitulate 12T-7f tumors *in vivo* would be advantageous in order to analyze the mechanisms by which stathmin influences prostate growth and tumor development. In this study, we used the NeoTag1 and NeoTag2 cell lines, which were established from tumors obtained by crossbreeding 12T-7f mice with ARR<sub>2</sub>PB-Neo mice to generate NeoTag bigenic mice. The establishment of the neomycin-resistant, Tag-expressing, cell lines is described in detail elsewhere (139).

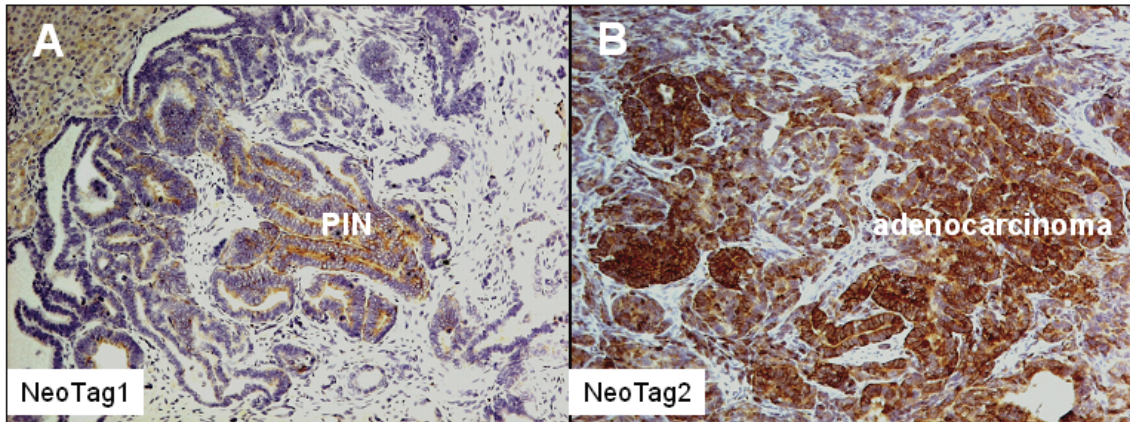


**Figure 12: Stathmin expression in NeoTag1 and NeoTag2 tumors generated by tissue recombination.** NeoTag1 and NeoTag2 cells (derived from 12T-7f tumors) were recombined with rat embryonic urogenital mesenchyme and grafted under the renal capsule. This model recapitulates the original 12T-7f tumors. Paraffin embedded sections were probed with rabbit anti-stathmin primary antibody and HRP-conjugated anti-rabbit IgG to detect stathmin expression.

Briefly, dorsolateral prostatic lobes from three 17-wk old ARR<sub>2</sub>PBneo x LPB-Tag male mice were dissected separately and cultured, generating three individual prostate epithelial cell lines designated as NeoTag1, NeoTag2 and NeoTag3. These prostate cell lines were cultured under 10<sup>-8</sup>M androgen selection and all NeoTag cell lines express the androgen receptor. In the tissue recombination assay, early passage NeoTag1 cells develop into prostate tumors, which primarily develop PIN with limited adenocarcinoma

lesions whereas NeoTag2 cells develop into tumors which contain primarily adenocarcinoma with some PIN. Thus, the tissue recombinants reconstitute a phenotype that is similar to the original 12T-7f tumors in that they develop PIN. However, they also show traits consistent with tumor progression (139).

In our study, NeoTag1 cells were selected to represent PIN lesions and NeoTag2 cells were selected to represent tumor progression. IHC analyses of NeoTag1 and NeoTag2 tissue recombinants were compared to determine whether stathmin expression increased with tumor progression. As per protocol described in the Materials and Methods section, NeoTag1 and NeoTag2 tissue recombinants were established by recombining 100,000 NeoTag1/2 cells with 250,000 rat embryonic UGM cells and grafting them under the renal capsule of adult male nude mouse hosts for 4 weeks. The resulting tumors were subjected to IHC analysis to identify the cell type that expressed stathmin and to determine whether stathmin expression increased in tumor progression from PIN to adenocarcinoma. Low levels of stathmin were observed in luminal epithelial cells of normal prostatic glands and stathmin expression increased in PIN lesions (Fig. 12 Panel A). In contrast, stathmin staining was most intense in adenocarcinoma lesions in NeoTag2 tumors (Fig. 12 Panel B), indicating that up-regulation of stathmin expression coincided with PCa progression.

### **Increased Stathmin Expression occurs in Human PCa**

To characterize stathmin expression in human PCa, we compared archival paraffin-embedded tissue sections containing PIN and adenocarcinoma adjacent to

benign prostate by IHC. In benign tissue, stathmin expression was primarily localized to the basal epithelial cells of prostatic glands (Fig. 13 panels a and b). Only a few luminal epithelial cells stained positive for stathmin within any given section. In PIN lesions, stathmin expression was predictably observed in basal epithelial cells; however its expression now strongly increased in luminal epithelial cells (Fig. 13 panels c and d). Double immunofluorescence staining with anti-p63 antibody, a basal epithelial cell marker, and anti-stathmin antibody further confirmed this pattern of expression in benign cells (Fig. 13 panels f, i and j) and PIN lesions (Fig. 13 panels h, k and l). The prostatic stroma was always found negative for stathmin staining.

Human prostate cancer is analyzed by the Gleason grading system for diagnosis and prognosis in the treatment of men with PCa. This system defines five histological patterns with decreasing differentiation ranging from Gleason pattern 1 which identifies a well circumscribed nodule of glands which does not infiltrate into adjacent benign prostatic tissue to Gleason pattern 5 in which there is an almost complete loss of glandular structure and epithelial cells invade the surrounding stroma. The most prevalent plus the second most prevalent patterns are added to obtain a Gleason score. We have available a prostate tissue microarray (TMA) which contains tissue cores representing BPH and Gleason patterns 3 through 5. The TMA consisted of 200 cores from a total of 50 BPH and PCa prostate biopsies (Table 1). IHC analysis using anti-stathmin antibody revealed that stathmin expression significantly increased in cores containing Gleason pattern 5 compared to cores containing Gleason pattern 4 ( $p < 0.05$ ), Gleason pattern 3 ( $p < 0.01$ ) and BPH ( $p < 0.05$ ) (Fig. 14). Thus, increased stathmin expression correlates with

the most advanced pattern of PCa.

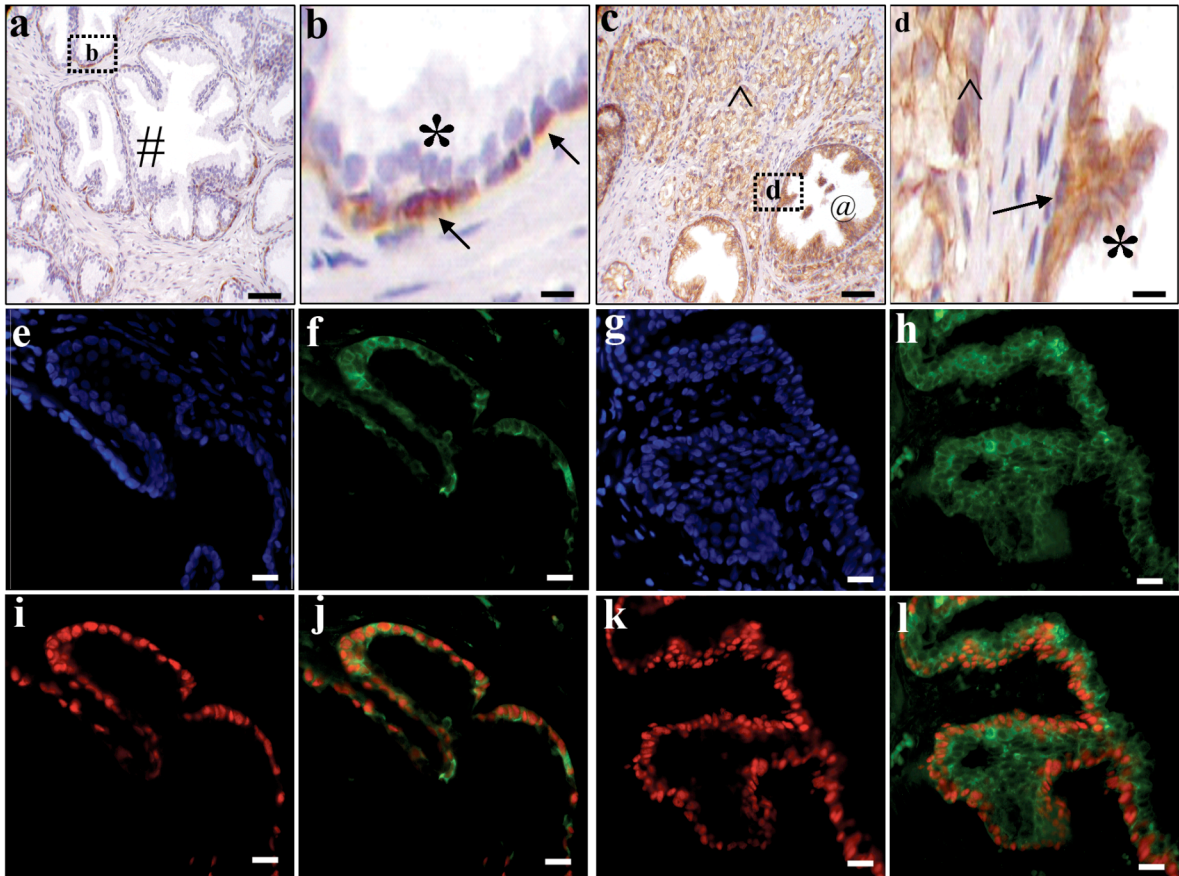
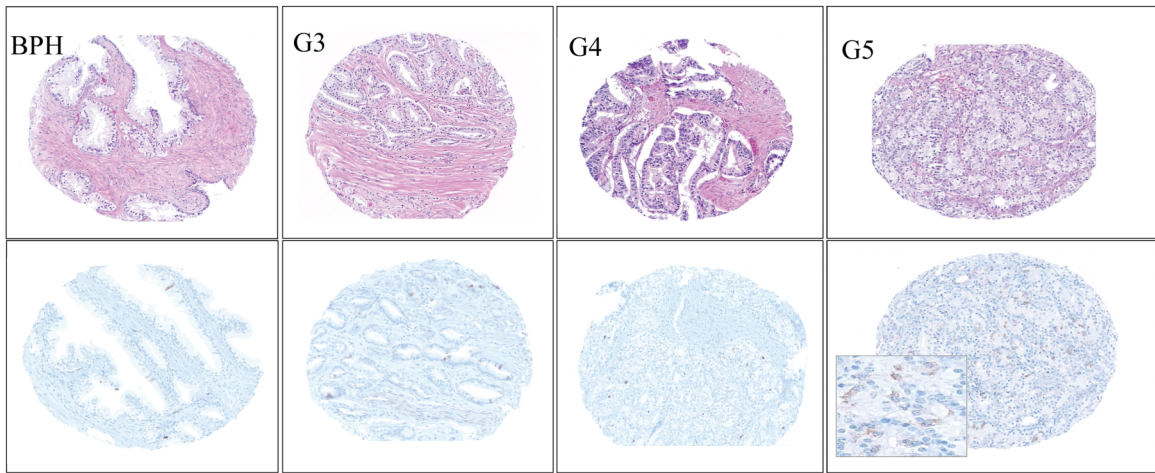


**Figure 13: Stathmin localization in benign human prostate and human prostate tumor tissue.** Paraffin embedded human prostate sections containing benign, PIN and adenocarcinoma lesions were stained with anti-stathmin antibody. Panel a, benign human prostate tissue. Scale 50µM. Panel b: Magnified region as indicated in Panel a. Scale, 10µM. Panel c, PIN and adenocarcinoma. Scale 50µM. Panel d, magnified region as indicated in Panel c. Scale, 10µM. # indicates benign prostatic hyperplasia (BPH); @, PIN; ^, adenocarcinoma. Arrows indicate basal epithelial cells and \*, luminal epithelial cells. Double fluorescence staining (Panels e-l) was performed to identify the cell type expressing stathmin. Archival human prostate tissue sections were stained with anti-stathmin and anti-p63 antibody. Secondary antibodies to detect stathmin and p63 were donkey anti-rabbit Alexa Fluor 488 (green) and donkey anti-mouse Alexa Fluor 594 respectively (red). Panels e (DAPI), f (stathmin), I (p63) and j (merged) represent benign prostate. Panels g (DAPI), h (stathmin), k (p63) and l (mergerd) represents PIN.

A



B

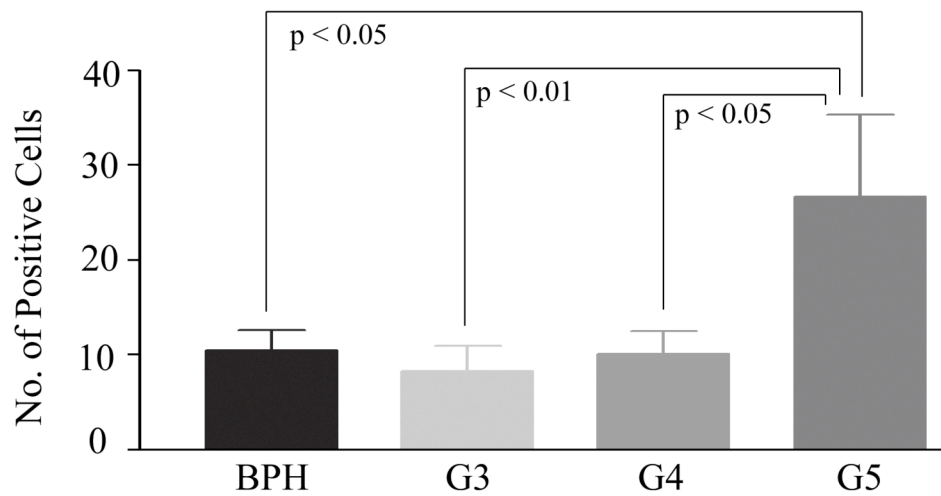


**Figure 14. Analysis of stathmin expression during human prostate cancer progression.** A human prostate tissue array containing samples arranged according to increasing Gleason pattern (see Table I) was analyzed to determine levels of stathmin expression. Panel A. Representative images of BPH, Gleason patterns 3, 4 and 5 human prostate specimens. Panel B. Stathmin expression was quantified by counting the number of stathmin positive cells per each core and the cores from each patient were averaged and graphed.

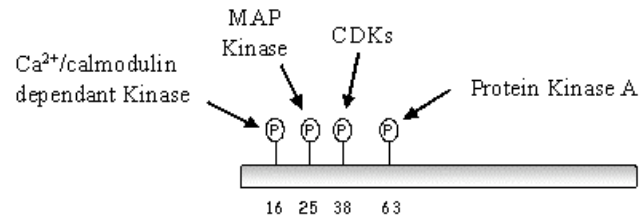
### **Stathmin is differentially expressed in androgen-dependent and androgen-independent PCa cell lines**

The observation that increased stathmin expression correlates with adenocarcinoma and local stromal invasion suggests that stathmin may play a role in tumor progression. Several cell lines that represent different aspects of advanced prostate cancer are available. These include the human PCa cell lines PC-3 and DU145 which do not require androgen for cell growth, the human LNCaP cell line which is androgen-sensitive and the mouse NeoTag1 and NeoTag2 cell lines which also require androgen for growth. These lines were tested by western blot analysis and densitometric values were normalized to GAPDH. Stathmin levels in androgen-independent PC-3 and DU145 cells were 6-fold and 4.5 fold higher ( $p < 0.05$ ) respectively, compared to those observed in androgen-sensitive LNCaP cells (Fig. 15B, densitometric data not shown). Thus increased stathmin expression correlated with androgen-independent cell growth. Furthermore, stathmin increased 1.5-fold in NeoTag2 cells compared to NeoTag1 cells (Fig. 15B), correlating with the IHC where NeoTag2 cells predominantly formed adenocarcinoma *in vivo* compared to NeoTag1 cells which develop primarily PIN lesions (Fig. 12).

### **Stathmin is Differentially Phosphorylated in Human and Mouse Prostate Cell Lines**

Stathmin contains 4 serines, Ser16, Ser25, Ser38 and Ser63, which are differentially phosphorylated to integrate different intracellular signals (Fig. 15A). We obtained 4 serine specific phospho-antibodies to compare stathmin phosphorylation levels in the PC-3, DU145, LNCaP, NeoTag1 and NeoTag2 cell lines. Cells were

A



B

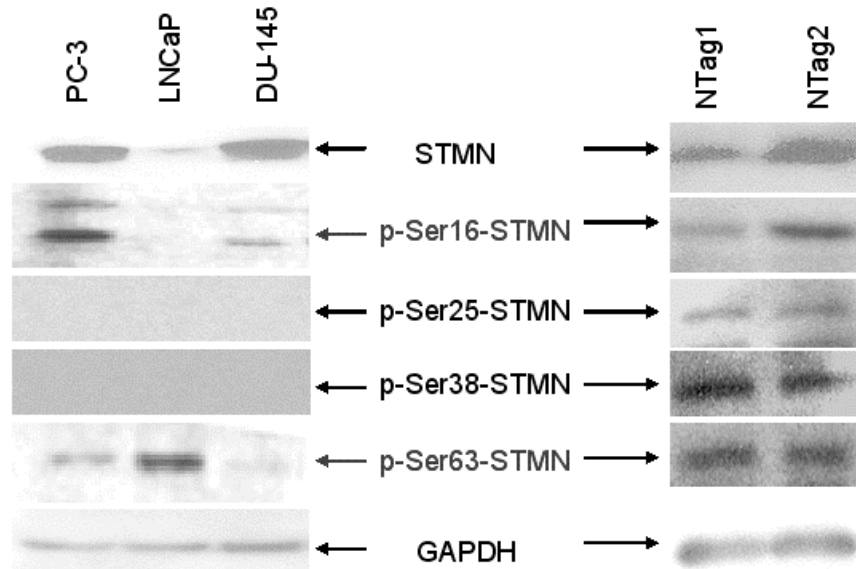


**Figure 15. Stathmin expression and phosphorylation at N-terminal serine residues in human and mouse prostate cell lines.** Panel A. Diagrammatic representation of the phosphorylation sites of stathmin at Ser16, Ser25, Ser38 and Ser63. Panel B. Western blot analyses of stathmin expression and phosphorylation using anti-stathmin antibody and antibodies specific to the four phospho-serines of stathmin. Stathmin is conserved in rodents and humans and therefore, the phospho-antibodies recognize their respective phosphorylated serines in both species. Androgen-independent PC-3 and DU145 cells, androgen-dependent LNCaP cells, mouse NeoTag1 and NeoTag2 prostate tumor cells were cultured as described in the Materials and Methods section. Twenty micrograms of protein were loaded per lane and the pattern of stathmin phosphorylation determined.

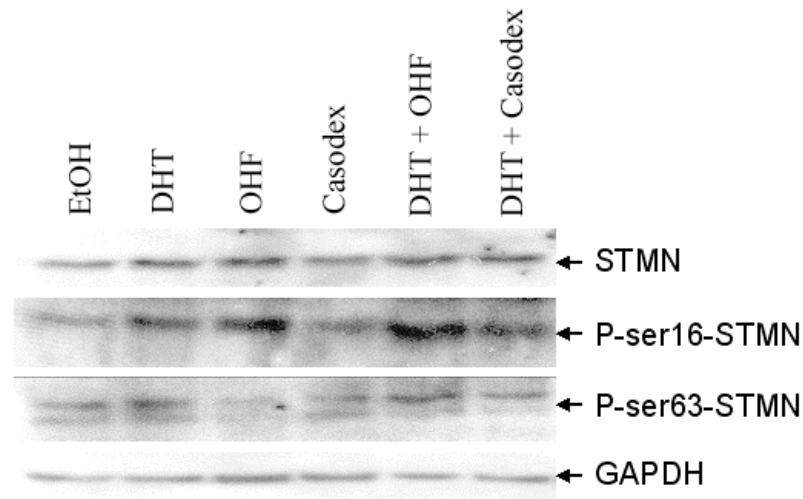


cultured in their respective medium as described in the Methods and Materials section, harvested and subjected to western blot analysis. As seen in Fig. 15B, stathmin was phosphorylated at Ser16 in PC-3 and DU145 with the highest levels observed in PC-3 cells. Little to no phosphorylated Ser16 was detected in LNCaP cells. Conversely, phosphorylated Ser63 was greatest in LNCaP cells compared to PC-3 and DU145 cells. Hence, phosphorylation at Ser16 seems to be prevalent in androgen-independent PCa cells whereas phosphorylation at Ser63 seems to be predominant in androgen-sensitive cells. Phosphorylation at Ser25 and Ser38 were not observed in these three cell lines. This is an important observation as it may enable us to elucidate molecular pathways differentially modulated by stathmin in androgen-dependent vs. androgen-independent state of the disease. In contrast, stathmin was phosphorylated at all 4 serines in the NeoTag1 and NeoTag2 cell lines, with phosphorylation at Ser16 being higher in NeoTag2 cells compared to that in NeoTag1 cells (Fig. 15B).

### **Androgens and Anti-androgens Modulate Stathmin Phosphorylation**

The differential phosphorylation of Ser16 in PC-3 and DU-145 cells and Ser63 in LNCaP cells suggest that stathmin may hold divergent roles in androgen-independent compared to androgen-dependent PCa. Androgens regulate normal prostate development and they promote the development of PCa. Even during androgen deprivation therapy when androgen levels are biochemically reduced, the androgen receptor (AR) signaling pathway may still be activated through other mechanisms (140). To elucidate which serine residues on stathmin were phosphorylated in response to androgen and anti-androgen treatment, AR-positive LNCaP cells were treated with vehicle (ETOH),

A



B

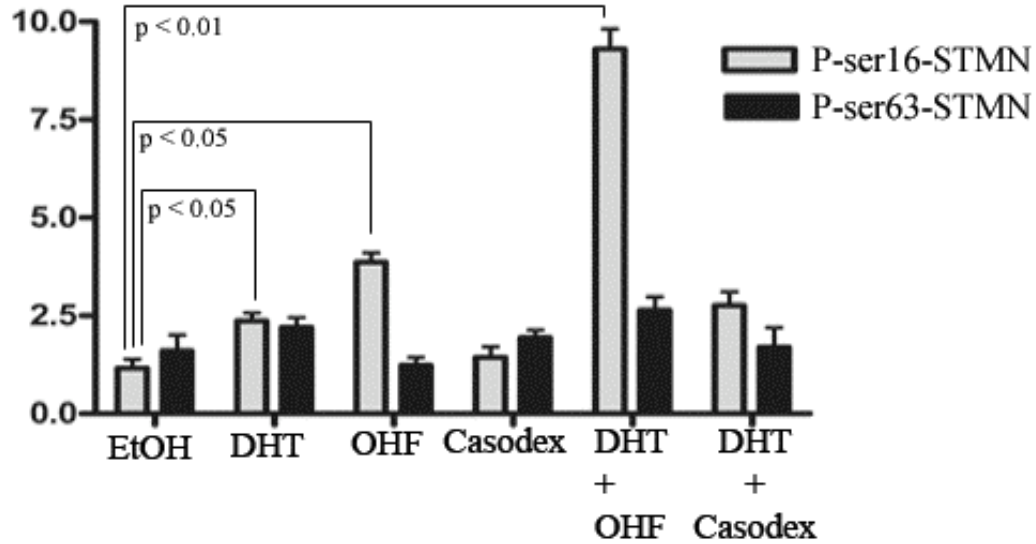


**Figure 16. Regulation of Stathmin phosphorylation by androgen and anti-androgen treatment.** Panel A. Western blot analysis of stathmin phosphorylation in response to androgen and antiandrogen treatment. LNCaP cells were treated with  $10^{-8}$  M dihydrotestosterone (DHT),  $10^{-8}$  M hydroxyflutamide (OHF),  $10^{-8}$  M Bicalutamide alone or in combination as indicated. Forty micrograms of protein were loaded per lane. Only Ser16 and Ser63 are presented since Ser 25 and Ser38 were not phosphorylated in PC-3, DU-145 or LNCaP cells. Panel B. Densitometric analysis of the western blot in Panel A. Analysis was performed utilizing ImageJ software and levels of serine phosphorylation were normalized to total stathmin normalized to GAPDH. This western blot analysis is representative of four separate experiments.

DHT ( $10^{-8}$ M), hydroxyflutamide ( $10^{-5}$ M), bicalutamide ( $10^{-5}$ M) or a combination of DHT and hydroxyflutamide or DHT and bicalutamide for 24 hours. Proteins were extracted and Ser16 and Ser63 phosphorylation was analyzed by western blot analysis.

Ser16 phosphorylation increased 2-fold with DHT treatment and 3.4-fold with hydroxyflutamide treatment (Fig. 16). The ligand-binding domain of the LNCaP AR contains a threonine to alanine point mutation at amino acid 877 (T877A) that allows hydroxyflutamide to function as an agonist (141). Thus, it is possible that phosphorylation of Ser16 increased through the agonistic activity of antiandrogen treatment. In presence of both DHT and hydroxyflutamide, Ser16 phosphorylation increased nearly 9-fold in LNCaP cells, indicating that DHT and hydroxyflutamide in combination resulted in a synergistic effect (Fig. 16). However, treatment with bicalutamide did not increase Ser16 phosphorylation over the EtOH control and did not cause a synergistic or additive effect in combination with DHT treatment. Interestingly, changes in Ser63 phosphorylation were not as pronounced as Ser16, increasing only 1.6-fold in response to DHT treatment and 1.8-fold in response to combination treatment of DHT and hydroxyflutamide treatment. The remaining treatment groups exhibited little or no induction in Ser63 phosphorylation (Fig. 16). These observations indicate that antiandrogen treatment up-regulates Ser16 phosphorylation in androgen-sensitive LNCaP cells, whereas Ser16 phosphorylation in androgen-independent (PC-3 and DU145) cells is already elevated in the absence of hormonal treatment (Fig. 16).

In summary, our study demonstrates that postnatally, stathmin expression is high

in prostatic epithelium and declines as the prostate differentiates into a growth quiescent gland. Stathmin expression is elevated again during PCa development and continues to be expressed during PCa progression. Analyses of archival human prostate tissue sections indicate that stathmin is initially expressed in the basal cell compartment in Benign Prostatic Hyperplasia (BPH), whereas stathmin is overexpressed in luminal epithelial cells in PIN and continues to be expressed in adenocarcinoma. Furthermore, differential stathmin phosphorylation is observed in androgen-independent PC-3 and DU145 cells compared to androgen-dependent LNCaP cells, suggesting that stathmin activity is modulated with PCa progression. Understanding which pathways stathmin regulate is imperative to identify potential targets for treatment of PCa.

**Table1. Tissue Array Representing BPH and PCa.** A total of 4 cores/patient or 200 cores from 50 BPH and PCa patients were arrayed in sequential order from Gleason Pattern 3 to 5.

Histopathology of Specimen	Number of Patients
BPH	12
Gleason Pattern 3	12
Gleason Pattern 4	10
Gleason Pattern 5	16
<b>Total</b>	<b>50</b>